Journal of Maps

ISSN: (Print) (Online) Journal homepage: https://www.tandfonline.com/loi/tjom20

Reconstructing anthropic coastal landscape of Campi Flegrei volcanic area (Southern Italy) during the Roman period from multi-technique surveys

Gaia Mattei, Lucio Amato, Claudia Caporizzo, Aldo Cinque, Gerardo Pappone, Alessia Sorrentino, Paolo Stocchi, Salvatore Troisi & Pietro P.C. Aucelli

To cite this article: Gaia Mattei, Lucio Amato, Claudia Caporizzo, Aldo Cinque, Gerardo Pappone, Alessia Sorrentino, Paolo Stocchi, Salvatore Troisi & Pietro P.C. Aucelli (2023): Reconstructing anthropic coastal landscape of Campi Flegrei volcanic area (Southern Italy) during the Roman period from multi-technique surveys, Journal of Maps, DOI: 10.1080/17445647.2023.2187320

To link to this article: https://doi.org/10.1080/17445647.2023.2187320

JOURNAL OF MAPS
https://doi.org/10.1080/17445647.2023.2187320

Reconstructing anthropic coastal landscape of Campi Flegrei volcanic area (Southern Italy) during the Roman period from multi-technique surveys

Gaia Mattei [a], Lucio Amato[b], Claudia Caporizzo [a], Aldo Cinque[c], Gerardo Pappone [a], Alessia Sorrentino [a], Paolo Stocchi [d], Salvatore Troisi [a] and Pietro P.C. Aucelli [a]

[a]Science and Technology Department, Università degli Studi di Napoli Parthenope, Naples, Italy; [b]Tecno-In S.p.A. - Engineering Services, Naples, Italy; [c]Earth Science Department, Università degli Studi di Napoli Federico II, Naples, Italy; [d]NIOZ Royal Netherlands Institute for Sea Research, Coastal Systems Department, Utrecht University, Den Burg, The Netherlands

ABSTRACT

Campi Flegrei is one of the widest and most dangerous active volcanic complexes in the Mediterranean basin, known to be affected by continuous and sudden vertical ground movements (bradyseismic crisis) that have characterized the post-calderic volcanic activity since the Late Pleistocene and particularly during the Roman period. Despite the intense volcano-tectonic processes, the area has been densely inhabited since the Greek-Roman as testified by several submerged archaeological remains here used as high-precision relative sea-level markers. By using a complex multi-technique approach made of direct, indirect morpho-acoustic and optical surveys, and stratigraphic analysis, we present a detailed reconstruction of the coastal landscape of Campi Flegrei and its surroundings between the Roman Late Republican and Early Imperial ages. The coastal scenario aims to facilitate the comprehension of how volcano-tectonic events influenced the evolution of this singular coastal landscape, and how these interfered with human activity in terms of damages and adaptation.

ARTICLE HISTORY
Received 12 September 2022
Revised 25 January 2023
Accepted 27 February 2023

KEYWORDS
Coastal landscape evolution; relative sea level; urban geomorphology; archeological sea-level markers; vertical ground movements; geomorphological analysis

1. Introduction

The coastal landscape of volcanic areas evolves as a result of the intimate interplay between volcanic activities and exogenous forcing. However, the climate-driven Holocene relative sea-level rise has interfered with their evolution producing a progressive submersion often exacerbated by subsiding trends of volcano-tectonic origin (Aucelli et al., 2020; Aucelli et al., 2021; Budillon et al., 2020; Mattei et al., 2022). In this context, Campi Flegrei is a complex volcanic system setting within a poly-caldera structure (Figure 1) formed as a consequence of two explosive super eruptions (the Campanian Ignimbrite dated at 39 ky BP by Isaia et al., 2016 and the Neapolitan Yellow Tuff dated at 15 ky BP by Deino et al., 2004) followed by three epochs of volcanic activity (15 - 10.6 ky BP, 9.6 −9.1 ky BP, and 5.5 - 3.5 ky BP, Smith et al., 2011 and references therein). The youngest phreato-magmatic eruption occurred in 1538 AD (Monte Nuovo; Di Vito et al., 1987).

The Campi Flegrei volcanic area has been characterized since the Early Holocene by sudden vertical ground movements (bradyseismic crisis) that have induced great modifications in inland areas and responsible of abrupt coastal changes (Aucelli et al., 2017a). Despite this volcano-tectonic activities, intense urbanization of the area occurred after the foundation in 194 BC of the Roman colony of *Puteoli* (located in the center of the modern Pozzuoli), which soon became the major commercial port of Rome.

During the Roman period, and in particular between the 1st century BC and the 1st century AD, an overall subsiding trend shortly interrupted by metric uplift (Aucelli et al., 2021) occurred in Campi Flegrei and its surroundings (Aucelli et al., 2019; Bellucci et al., 2006; Cinque et al., 1997; Morhange et al., 2006; Pappalardo & Russo, 2001; Passaro et al., 2013; Troise et al., 2007), causing sensible coastline modifications that induced adaptation reactions well proved by archaeology. For example, in 12 BC the Roman military fleet had to be definitely outscored from *Portus Julius* (built in 37 BC) to *Portus Misenum* (i.e. port of Miseno), outside the unstable caldera (Passaro et al., 2013). Another example comes from the *Macellum* building of Pozzuoli (Figure 1), whose ground floor (constructed in the 2nd century BC) finished under the sea level and, afterward, was reconstructed about 2 m higher around 80 AD (Dvorak & Mastrolorenzo, 1991; Levi, 1969).

The overall subsidence reached its maximum between 334–527 A.D, and 1336–1454 A.D. as proved by the *Lithophaga* perforations visible at about 7 m asl

CONTACT Claudia Caporizzo claudia.caporizzo@collaboratore.uniparthenope.it
Supplemental data for this article can be accessed online at https://doi.org/10.1080/17445647.2023.2187320.

Figure 1. Geological and geomorphological map of the study area (after Ascione et al., 2020).

on the still-standing columns of the Roman market (14C dating in Morhange et al., 2006) in Pozzuoli.

Even if this tectonic behavior inverted its trend after the Monte Nuovo eruption, the Roman seascape between Baia and Naples, passing through Pozzuoli, is presently still submerged (Figure 1, red polygons).

We surveyed all the submerged archaeological remains of Roman Age (Figure 1, red polygons) in order to study the effect of volcanic and volcano-tectonic events on the evolution of the coastal landscape of this active volcanic area, reconstructing damages and human adaptation (Aucelli et al., 2017b) related to the abovementioned landmass movements.

The map aims to propose a paleo-geographic reconstruction of the period of maximum Roman urbanization between the 1st century BC and the 1st century AD obtained by overlying new data from our surveys and geoarchaeological data described in the previous studies (Bellucci et al., 2006; Dvorak & Mastrolorenzo, 1991; Morhange et al., 1999; Morhange et al., 2006; Todesco et al., 2014) in order to provide new knowledge on the effects of a volcano-tectonic subsiding trend on the accelerated sea-level rise due to the ongoing climate change, in terms of coastal modification and consequent human adaptations.

2. Methods

In this study, a multi-method approach including direct and indirect methods (Figure 2) was applied to the main coastal sectors with submerged or semi-submerged archaeological structures of the Roman

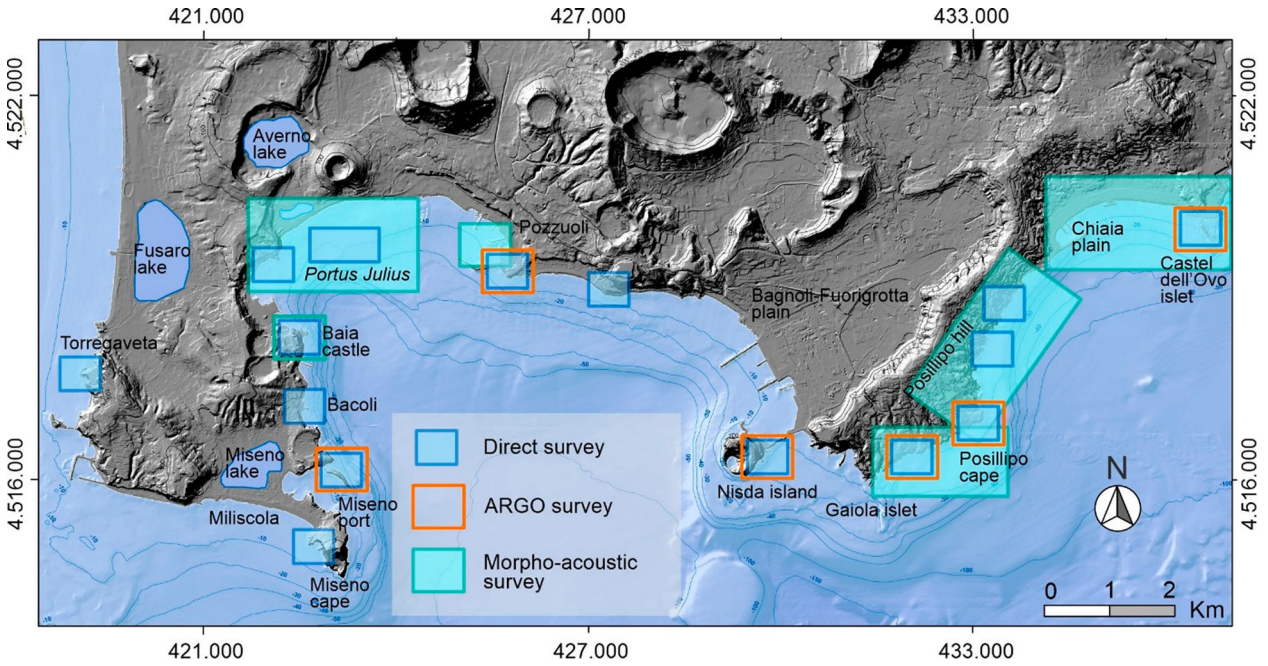

Figure 2. A. Map of the study area with the distribution of the different surveys carried out along each coastal sector with archaeological structures.

age, in order to obtain an extensive mapping of the ancient coastal landscape. In particular, data from detailed direct surveys were overlaid with new coring data, photo-interpretation, morphometric analysis of high-resolution Digital Terrain Models (DTMs) from Lidar and bathymetric data, and analysis of morpho-acoustic and optical data measured with different instruments.

2.1. Morphoacoustic surveys

The 34% of coastal sectors were surveyed through a multibeam echo sounder (MBES) system equipped with a SeaBat7125 sonar (400 kHz; Caporizzo et al., 2021). The acquired bathymetric data were processed using the Teledyne PDS editing module, corrected for the tidal datum, and finally elaborated in the ArcGIS environment to calculate a high-resolution DTM of the seafloor (0.25 × 0.25 m cell size).

In specific sectors with sufficient bathymetry and a high presence of archaeological structures, an acoustic mapping of the seabed was carried out by a GeoAcoustics dual-frequency (114/410 kHz) SSS (Side Scan Sonar) system (MOD259). The derived sonographs were combined in a mosaic and subjected to backscattering analysis to define the different nature of the targets and their morphological characterization.

2.2. ARGO system (SSS, SBES, photogrammetric survey)

The survey of critical areas, due to shallow water conditions and the presence of semi-submerged archaeological structures, was carried out with a prototype of unmanned surface vessel (USV). ARGO project is a framework of sub-systems, resulting from an open-prototyping project applied to underwater geoarchaeological research (Mattei et al., 2018a; Mattei et al., 2020a). This small catamaran-like drone (1.20 × 0.86 m; Figure 3) follows a modern multimodal mapping approach involving the simultaneous and integrated use of both optical and geo-acoustic sensors. The geo-acoustic sensors are a single-beam echo sounder (SBES, Ohmex SonaLite) with 200 kHz acquisition frequency and 80 m as maximum measured depth and a sides scan sonar (Sonar Tritech Side-Scan StarFish 450C) optimized for coastal waters (450 kHz CHIRP transmission). These instruments are embedded in the USV with an offset of a few centimeters from the GPS. The photogrammetric system consists of two Xiaomi YI Action cameras placed parallel with the vertical axis, with a variable stereoscopic base chosen in relation to the bathymetry of the study area and a GoPro Hero 3 forming an angle of about 30 with the seabed. The transmission of all acquired data in broadcasting allows the simultaneous work of a multidisciplinary team of specialists able to analyze specific datasets in real-time.

2.3. Direct surveys

The direct surveys carried out in this study included extensive geological and geomorphological on-field observations, often supported by archaeological interpretations done by a team of experts in geoarchaeological underwater surveys.

Along the submerged sector of the study area, several underwater geo-archaeological surveys were

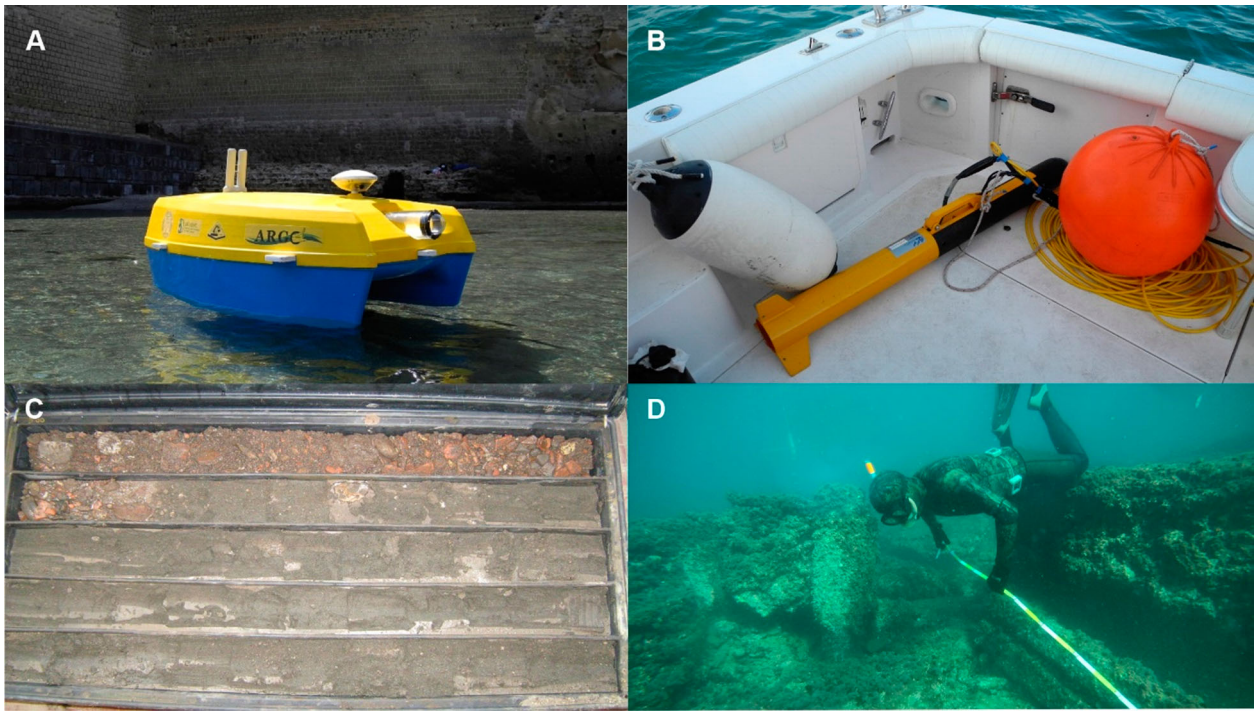

Figure 3. Photos of: A) Argo marine drone in action during a survey performed along the coastal sector around Castel dell' Ovo; B) SSS transducer during the survey at Baia; C) Borehole drilled at Pozzuoli; D) Direct survey at Portus Julius.

performed by a multidisciplinary team of specialized scuba divers aiming at interpreting the underwater landscape and detecting the submersion measurements of different archaeological sea-level markers (SLMs, red polygons in Figure 1) using a level staff or a depth gauge. The submersion measurements were corrected with respect to the water tidal level and used for the determination of past sea-level positions.

2.4. Stratigraphic analysis

The archaeo-stratigraphic records analyzed in this paper were reconstructed by overlying data from previous studies of the low-lying coastal areas and new data from geoarchaeological excavations made by TecnoIn Spa in the last 20 years. Particular attention was paid to the recognition of anthropogenic intervals (i.e. loose mixture of yellow tuff slabs and mortar related to masonry works) and to the recovery of all the archaeological remains (such as pottery and mosaic fragments) present in some littoral strata. This was aimed to chronologically constrain those strata establishing the *ante-* and *post-quem* time relationships between the strata. The sedimentary succession of the analysed boreholes (positioned in both main maps) provided crucial information to reconstruct the coastal environments between the 1st century BC and 1st century AD.

2.5. Spatial data analysis

All data collected from the direct and indirect surveys and archaeo-stratigraphic interpretations were managed in a GIS environment (Amato et al., 2018) and overlaid with emerged-submerged DTMs. In particular, while the elevations of the emerged sector derived from LIDAR data provided by the Ministry of Environment, bathymetric data in the map stem from the CARG project by Campania Region. In both cases, the altimetric datasets were interpolated by using a Topo to Raster interpolator to obtain two accurate DTMs for the emerged and submerged sectors with a cell size resolution of 2×2 m and 5×5 m, respectively. The coastal area was investigated in order to reconstruct the coast morphology between the 1st century BC and 1st century AD, consequently, evaluating the overall coastal retreat/progradation trend affecting the area. Spatial modifications in each coastal sector were calculated by combining the geomorphological interpretations and the archaeological evidence interpreted both as a witness of the ancient coastal landscape and as relative-sea-level (RSL) markers of high precision.

The internal area of the emerged DTM and the deep sectors of the underwater one did not undergo any changes, except for the Monte Nuovo area where the cone was removed having formed during the eruption of 1538 AD.

2.6. Archaeological sea-level markers

According to Table 1, based on their direct/indirect relationship with the former sea level, the archaeological SLMs identified in this research can be classified as terrestrial limiting points (TLPs), useful for the

Table 1. List of sea-level markers (SLMs) identified in the study area: SLM type (sea-level index point – SLIP or terrestrial limiting point – TLP; column 1); interpreted archaeological feature (column 2); Functional clearance (FC expressed in meters; column 3); Indicative Range (mean high water – MHW, mean low water – MLW, medium sea level – MSL; column 4); Examples of different markers identified through their ID-number which pictures are presented in the main maps (Map 1 – from Fusaro Lake to Nisida, and Map 2 – from Nisida to Municipio Plain; column 5).

Type	Feature	FC	IR	ID Maps
SLIP	Top sluice gate – fish tank	0.2	from MHW to MLW	#05 Map1
SLIP	Lower crepido – fish tank	0.2	from MHW to MLW	#01 Map1 #29 Map2
SLIP	Concrete change – pier	0.5	from MHW to MLW	#13 Map1 #18, #26 Map2
TLP	Pavement – building	above former MSL	above former MSL	#08, #10 Map1 #20, #23, #28 Map2
TLP	Top breakwater – infrastructure	above former MSL	above former MSL	#11 Map1

establishment of the upper limit of the former sea-level position (i.e. buildings and/or infrastructure remains as pavements and paved roads), and high precision sea-level index points (SLIPs; i.e. *crepido* and sluice gates of fish tanks and/or concrete change detection in roman *pilae*).

In particular, in the case of a SLIP the position of the ancient sea level can be calculated as follows:

$$SLIP = A - FC - \frac{IR}{2}$$

where A is the elevation above MSL, FC is the functional clearance (i.e. specific minimum elevation of each structure above the MSL at the time of its construction; Aucelli et al., 2020; Aucelli et al., 2021; Mattei et al., 2020b) and IR is the Indicative range (i.e. elevation range over which the marker forms; Shennan, 2015).

The RSL data derived from the archaeological SLMs were compared with a certain number of glacial- and hydro-isostatic adjustment (GIA) models specifically created for the study area (Mattei et al., 2022) in order to isolate the GIA-driven RSL component from the volcano-tectonic one.

In this regard, a suite of RSL curves were produced by using the sea level equation solver SELEN (Spada & Stocchi, 2007) coupled with three ice-sheet models (ICE-5 G, Peltier, 2004; ICE-6 G, Peltier et al., 2015; ANICE-SELEN, de Boer et al., 2014). The sea-level equation has been solved for a total of 54 models assuming different values for both the lithosphere thickness and the lower and intermediate mantle viscosity. Finally, the vertical displacement related to each SLM was calculated in a Python environment (Spyder – Anaconda3) through the use of a Bayesian statistical approach implying Monte-Carlo simulations (Mattei et al., 2022 and references therein).

3. Results and discussion

The identification of numerous archaeological SLMs along the whole coastal sector (Tables 2–4) and their integration with bibliographic sources (Paoli, 1768; Guadagno, 1994; Amato et al., 2000; Buonaguro, 2008; Camodeca, 2011; Gianfrotta, 2011) and geomorphological field data, allowed the reconstruction of the map of the Roman coastal landscape of Campi Flegrei and its surroundings providing crucial information on the main morphoevolutive prograding/retreating trends in the last 2000 years.

In general, the coastal landscape of the Campi Flegrei and its surroundings are characterized by rugged tufaceous sea cliffs alternated with small bays, occasionally hosting narrow coastal plains. During the Roman period, this fascinating scenario was strongly and continuously modified by the sustained interplay between human interventions, GIA, volcano-tectonic subsidence and sloping, and alluvial and coastal processes.

In particular, the inner Campi Flegrei caldera (Main Map 1) was bordered by active sea cliffs. However, the coastal sector between Baia and Miseno (Main Map 1) was characterized by raised paleoshore platforms, probably shaped during the 3rd eruptive epoch (5.5 - 3.5 ka BP, Smith et al., 2011), when a decametric subsidence and Late Holocene GIA-driven RSL rise (Isaia et al., 2019) produced the flooding of the whole Neapolitan Yellow Tuff caldera. Several Roman coastal structures such as ports, fish tanks, and *nymphaeums* were laid on sub-horizontal

Table 2. Sea-level markers (SLMs) identified in the coastal sector ranging from Fusaro Lake to Miseno Cape: SLM ID (column 1); Age (expressed in ka BP, column 2); SLM type (sea-level index point – SLIP or terrestrial limiting point – TLP; column 3); interpreted archaeological feature (column 4); RSL and related uncertainty (expressed in meters, column 5); vertical displacement and related uncertainty (VD; expressed in meters, column 6); Source (column 7). Data from Mattei et al., 2022.

ID	Age	SLM	Feature	RSL ± 2σ	VD ± 2σ	Source
#01	2.00	SLIP	Top sluice gate - fish tank	−3.3 ± 0.29	−2.56 ± 0.46	New data
#02	2.00	TLP	Pavement – building	<−2.69 ± 0.07	–	New data
#03	2.01	SLIP	Lower crepido – fish tank	−3.20 ± 0.29	−2.47 ± 0.45	Mattei et al. (2022)

Table 3. Sea–level markers (SLMs) identified in the coastal sector ranging from Miseno Cape to Nisida: SLM ID (column 1); Age (expressed in ka BP, column 2); SLM type (sea–level index point – SLIP or terrestrial limiting point – TLP; column 3); interpreted archaeological feature (column 4); RSL and related uncertainty (expressed in meters, column 5); vertical displacement and related uncertainty (VD; expressed in meters, column 6); Source (column 7). Data from Mattei et al., 2022.

ID	Age	SLM	Feature	RSL ± 2σ	VD ± 2σ	Source
#04	1.97	SLIP	Top sluice gate – fish tank	−4.20 ± 0.29	−3.49 ± 0.45	Aucelli et al. (2021)
#05	2.01	SLIP	Top sluice gate – fish tank	−4.00 ± 0.29	−3.27 ± 0.45	Aucelli et al. (2021)
#06	2.02	SLIP	Top sluice gate – fish tank	−4.20 ± 0.29	−3.30 ± 0.44	Aucelli et al. (2021)
#07	2.05	TLP	Top breakwater – infrastructure	<−5.80 ± 0.07	–	Mattei et al., (2022)
#08	1.84	TLP	Pavement – building	<−6.10 ± 0.07	–	Mattei et al., (2022)
#09	1.87	SLIP	Top sluice gate – fish tank	−6.90 ± 0.29	−6.22 ± 0.43	New data
#10	1.90	TLP	Pavement – building	<−5.30 ± 0.07	–	Mattei et al., (2022)
#11	2.25	TLP	Top breakwater – infrastructure	<−7.00 ± 0.07	–	New data
#12	1.96	SLIP	Top sluice gate – fish tank	−3.10 ± 0.29	−2.40 ± 0.44	Aucelli et al. (2020)
#13	1.98	SLIP	Concrete change – pier	−3.10 ± 0.29	−2.38 ± 0.45	Aucelli et al. (2020)
#14	2.02	TLP	Pavement – building	<−5.20 ± 0.05	–	Aucelli et al. (2020)
#15	1.84	TLP	Pavement – building	<−4.50 ± 0.07	–	New data
#16	1.84	TLP	Pavement – building	<−4.00 ± 0.07	–	New data
#17	1.97	TLP	Concrete change – pier	<−3.00 ± 0.07	–	New data

platforms originated by the combined action of wave erosion and tuff quarrying.

Similarly, also the gently sloped sea cliff along the outer margin of the Campi Flegrei caldera, like those of the Posillipo sector (Main Map 2), appeared bordered by narrow shore platforms, sculptured during the Late Holocene RSL rise where *pilae*, fish thanks and breakwaters were built.

Despite overall subsidence with differential rates affecting the whole study area, the coastline of the low-lying sectors was pushed several tens of meters seaward by the casting of anthropogenic infillings, as in the case of the Portus Julius neighborhood (Main Map 1), or stabilized by the construction of ports, villas, and roads, as the case of Chiaia-Municipio plain (Main Map 2). The intense human occupation of Campi Flegrei and its surroundings lasted until the 5th century AD when the fall of the Roman Empire coincided with accelerated subsidence inside the caldera, which produced a RSL rise up to +7 m MSL and consequent coastal flooding that lasted some centuries. On the other hand, almost at the same time, in Naples, the '*Neapolis* Port' was buried by the huge pyroclastic fall related to the sub-Plinian Vesuvius eruption occurred in 472 AD.

In the following sections, the coastal landscape reconstructed in each of the two 1:20.000 maps is described in detail.

3.1. From Fusaro Lake to Rione Terra – Map 1

During the 1st century BC, the coastal stretch between the ancient *Acherusia Palus* (i.e. Fusaro Lake) and Miseno Cape was characterized by an alternate of high- and low-coast sectors. In particular, the shoreline near the Fusaro lake was constituted by a low coast with a length of about 3.0 km and made of a spit sandy barrier (*Strabo, Geographica V*) with a width of about 0.18 km laying between the coastal lagoon and the open sea (De Pippo et al., 2007). According to Seneca (*Epistula, LV, 2*) and Strabo (*Geographica, V*), the spit went through a very fast growth that lasted only 40 years and extended towards Torregaveta Promontory, recording an overall coastal progradation of about 0.2 km during the last 2.0 ka.

Starting from Torregaveta headland (Figure 4C), a high coast sector reaching a maximum elevation of 100 m extends for about 4.0 km. Here the coastal landscape was characterized by the presence of the

Table 4. Sea–level markers (SLMs) identified in the coastal sector ranging from Nisida to Municipio coastal plain: SLM ID (column 1); Age (expressed in ka BP, column 2); SLM type (sea–level index point – SLIP or terrestrial limiting point – TLP; column 3); interpreted archaeological feature (column 4); RSL and related uncertainty (expressed in meters, column 5); vertical displacement and related uncertainty (VD; expressed in meters, column 6); Source (column 7). Data from Mattei et al., 2022.

ID	Age	SLM	Feature	RSL ± 2σ	VD ± 2σ	Source
#18	1.95	SLIP	Concrete change – pier	−3.10 ± 0.21	−2.40 ± 0.39	Mattei et al. (2018b)
#19	1.95	SLIP	Top sluice gate – fish tank	−3.00 ± 0.28	−2.29 ± 0.44	Aucelli et al. (2019)
#20	1.97	TLP	Pavement – building	<−4.40 ± 0.07	–	Aucelli et al. (2018)
#21	1.97	SLIP	Concrete change – pier	−4–4 ± 0.50	−3.68 ± 0.60	Aucelli et al. (2018)
#22	1.95	SLIP	Concrete change – pier	−2.90 ± 0.50	−2.19 ± 0.60	Aucelli et al. (2019)
#23	1.95	TLP	Pavement – building	<−3.20 ± 0.07	–	Aucelli et al. (2019)
#24	1.95	SLIP	Concrete change – pier	−2.0 ± 1.00	−1.30 ± 1.05	Aucelli et al. (2019)
#25	1.95	SLIP	Concrete change – pier	−2.40 ± 1.00	−1.69 ± 1.05	Aucelli et al. (2019)
#26	1.97	SLIP	Concrete change – pier	−5.0 ± 1.00	−4.29 ± 1.05	Aucelli et al. (2019)
#27	1.95	TLP	Pavement – building	<−3.5 ± 0.07	–	Aucelli et al. (2019)
#28	1.97	TLP	Pavement – building	<−4.5 ± 0.07	–	Aucelli et al. (2019)
#29	2.00	SLIP	Lower crepido – fish tank	−2.2 ± 0.21	−3.78 ± 0.35	Pappone et al. (2019) Mattei et al., (2020b)

Figure 4. A. Semi-submerged archaeological remains of Vatia Villa at Torregaveta; B. detail of the fish-tank complex remains at Lucullus Villa along the western side of Miseno Cape; C. View from the south of Torregaveta Promontory; D. View of the sea cliffs of Monte di Procida.

maritime villa belonging to the console *Publius Servilius Vatia Isauricus* (*Seneca, Epistula, LV*; Caputo, 2006; Figure 4A) with the annexed fish tank and *nymphaeum* (ID#01-02, Table 2). Behind the fish tank, a rocky platform of mixed natural and anthropic origin, with an extension of about 50-60 m, emerged, cut by a series of connected channels. Due to the presence of these archaeological findings and their interpretation,

it was possible to assess an overall sea cliff retreat for the last 2.0 ky of about 0.13 km.

Moving forward, southeast from Monte di Procida seacliff (Figure 4D), the low-coast stretch of Miliscola beach extended for 1.8 km, with a maximum width of about 0.18 km, up to Capo Miseno headland. The latter, made of high rocky coast with a maximum height of 160 m, was characterized by the presence on its western side, nearby the Dragonara Cave, of a complex of fish tanks historically attributed to the Roman politician *Lucullus* (Figure 4B; Benini et al., 2008; ID#03, Table 2). From the 1st century BC, while by Miliscola beach the coastal sector was affected by a prevailing coastal progradation of about 0.13 km, at Miseno Cape, a slight coastal retreat of 0.04 km has been recorded with peaks along its western side of about 0.08 km.

The coastal stretch extending from Miseno Cape up to Nisida Island was one of the sectors more interested in extensive coastal anthropisation testified by an uninterrupted presence of archaeological findings (Busen, 2016).

Ranging from the eastern side of Miseno Cape to the northern sector of Punta Pennata Island, the area was characterized by a high rocky coast with a length of about 2.5 km, except for the small bay occupied by *Portus Misenum* (i.e. Miseno Harbour; Paget, 1971). The inlet was bordered to the south by the rocky spur of Punta Terone, where a fish tank was present at the time probably related to a maritime villa constructed before the military harbor at the end of the 1st century BC (ID#04, Table 3), and it was connected with the innermost *Lacus Misenum* (i.e. Miseno Lake) by an artificial channel (Iliano, 2017). On the opposite side, Punta Pennata (Figure 5A; Maiuri, 1963; Iliano, 2017) hosted a maritime villa built in the 1st century AD with some rooms on a paleo-shore platform emerged at that time (Benini & Lanteri, 2010).

During the last 2.0 ka, this sector was characterized by a general coastal retreat with a peak of 0.28 km recorded within Miseno Bay and much lower values of about 0.04 km along the eastern margin of Miseno Cape and the high coast protracting for 1.2 km north from Punta Pennata Island, connected to the mainland during the 1st century BC (Aucelli et al., 2021).

Heading north, from Garibaldi dock up to Baia Castle (Figure 5B), the coastal landscape of the 1st century BC was mainly characterized by the presence of a paleo-seacliff bordered by an emerged platform most likely enlarged by anthropogenic action (nowadays totally submerged) that is the evidence of a general coastal retreat of about 0.1 km occurred in a period preceding the Roman occupation. Along this coastal sector, several thermal baths (resting on the platform) and maritime villas were built (Miniero, 2010a; Guidone et al., 2017, Iliano, 2017), as presently testified by the remains of a fish tank related to the *Hortensius Hortalus* Villa (ID#05, Table 3; Di Fraia, 1993) and that of a fish tank interpreted as a part of *Caesar*'s domains (ID#06, Table 3; Miniero, 2010b).

North of Baia Castle, the landscape during the 1st century BC was strongly anthropized and bordered to the East by the ancient port inlet of *Lacus Baianus* (ID#07, Table 3; Maniscalco, 2004; Brandon et al., 2008). This sheltered embayment is the result of marine erosion on the emerged flanks of the Fondi di Baia volcano. The area hosted numerous luxurious buildings such as Protiro Villa (Di Fraia, 1993), *Pisonis* Villa with its thermal complex and fish tank system (Di Fraia et al., 1986; Di Fraia, 1993; Passaro et al., 2013), and *Claudius Nymphaeum* (Benini, 2004; Lombardo, 2009) at Punta Epitaffio (Figure 5C; ID#08-10, Table 3).

At the time, a huge breakwater nowadays improperly ascribed to the *Via Herculanea* (ID#11, Table 3) was built on nearshore sediments extending NE from *Pisonis* Villa for 1.2 km and isolating the ancient *Lacus Lucrinus* (i.e. Lucrino Lake) from the open sea. The breakwater was interrupted in the central part by the entry channel of *Portus Julius*, one of the most important infrastructures of the time in which several remains (ID#12-14, Table 3), including a well-preserved fish tank, and several *pilae* and buildings (i.e. a maritime villa of the beginning of the 1st century BC and numerous warehouses; Gianfrotta, 2012).

In particular, during the 1st century BC, the *Lacus Lucrinus* was a closed lagoon wider than the present day, used for oyster farming, and connected through an artificial channel to the innermost *Lacus Avernus* (i.e. Averno Lake), a volcanic crater formed during the 3rd eruptive epoch of Campi Flegrei (4.1 ka BP, Smith et al., 2011). Eastward, the plain was strongly modified by an artificial infill (Amato & Gialanella, 2013) that produced an average 200-meter coastal progradation on which the harbor districts of *Vicus Annianus* and *Vicus Lartidianus* (ID#15-16, Table 3) were built.

In general, the strongly anthropized coastal sector experienced an overall coastal retreat with maximum values of 0.5 km mainly related to the Middle Age subsidence that brought the RSL up to 7 m MSL (Morhange et al., 2006).

Finally, the 370-m long Molo Caligoliano and its numerous *pilae* (ID#17, Table 3; Camodeca, 1994) were built in that years at the foot slopes of the ancient tuff cone of Rione Terra (Figure 5D), where the Roman colony of *Puteoli* was established in 194 BC.

3.2. From Rione Terra to Municipio Plain – Map 2

Ranging from Rione Terra to Bagnoli-Fuorigrotta plain, the area was characterized by 3.0 km of high coast followed by a 2.7-km long sector of sandy low-

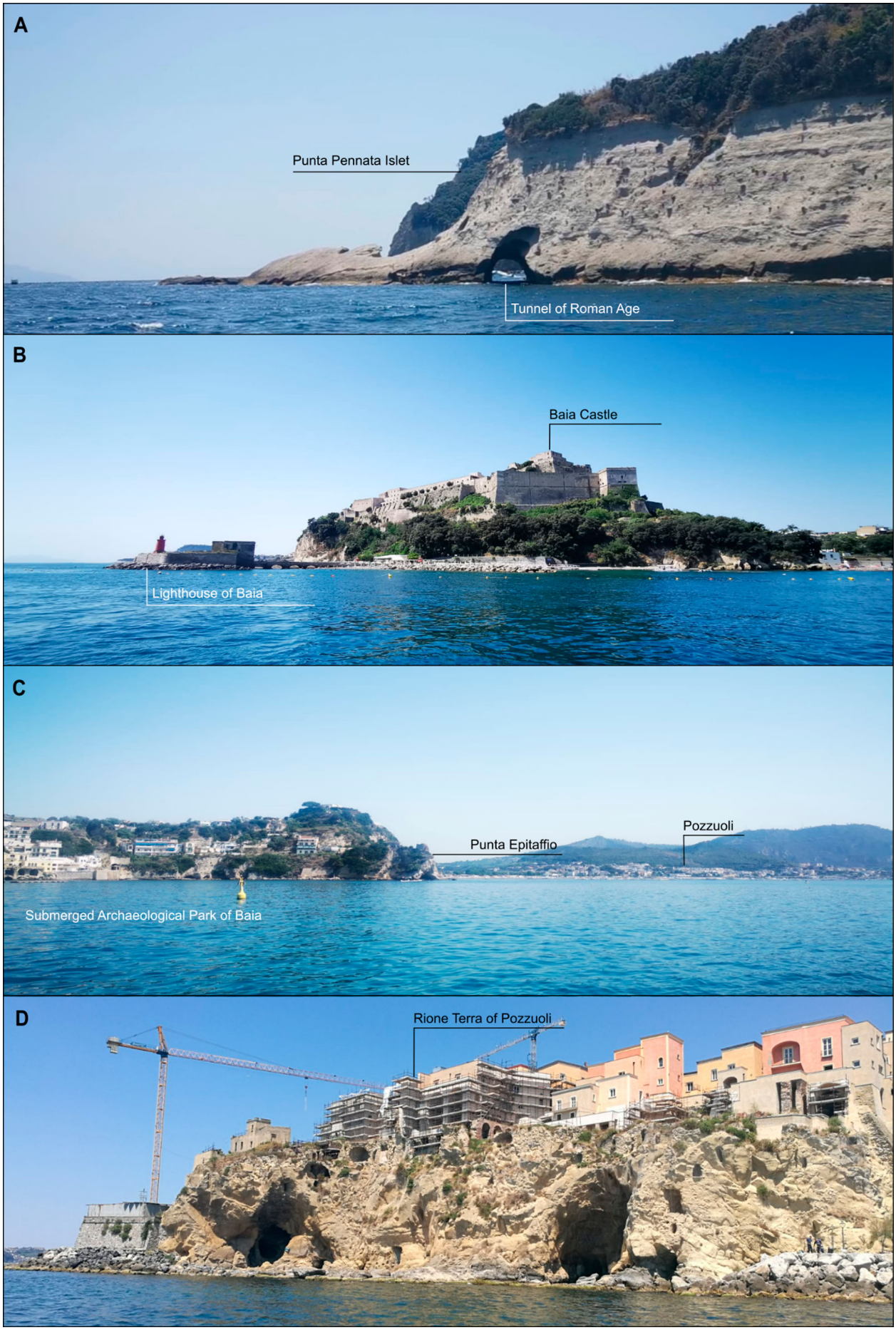

Figure 5. A. The southern side of the Island of Punta Pennata and one of the three Roman tunnels that pass through it; B. View from the north of Baia Castle; C. View from the south of Punta Epitaffio; D. View from the sea of Rione Terra in Pozzuoli.

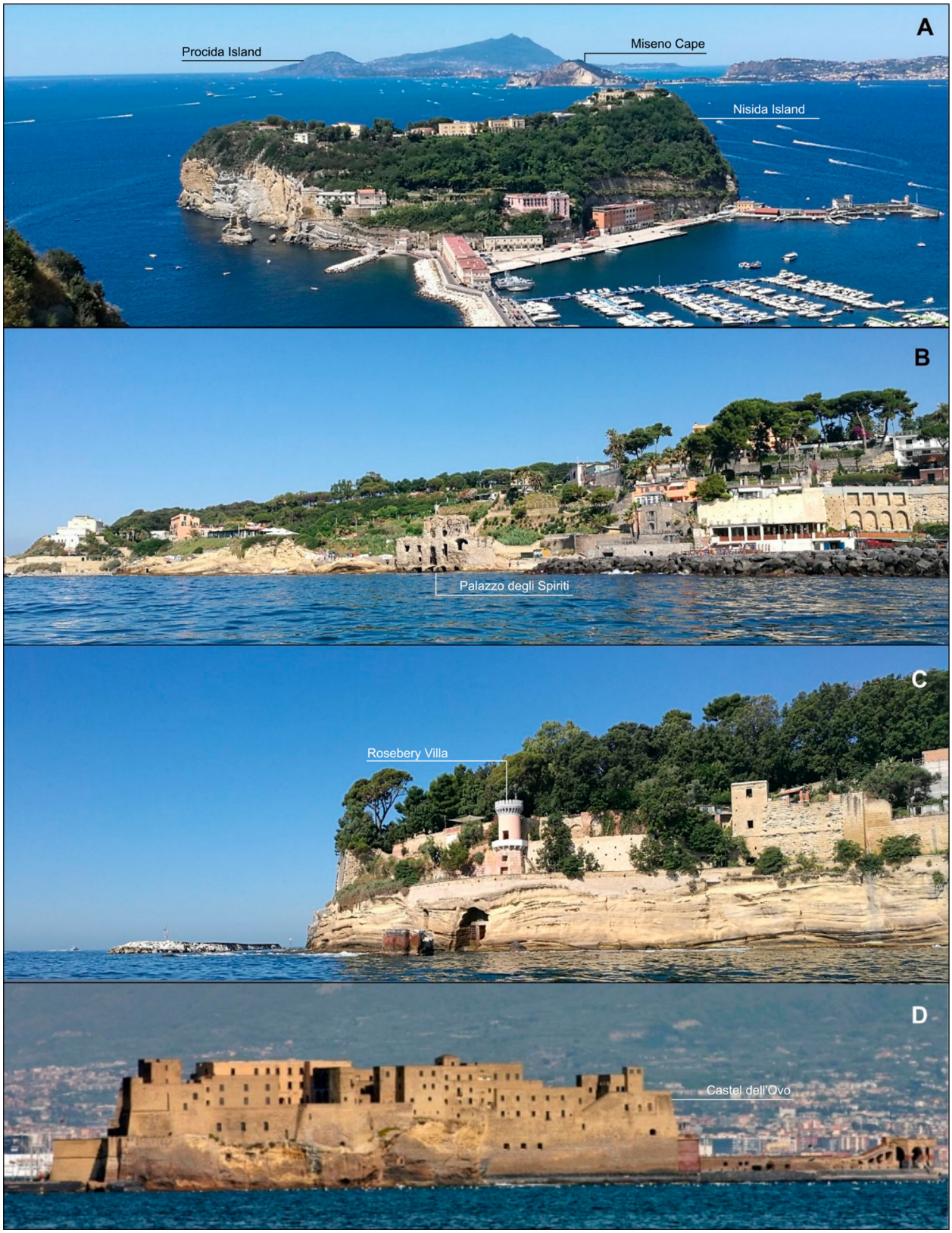

Figure 6. A. View from NE of Nisida Island; B. View from the sea of Posillipo coast with the famous palazzo degli Spiriti in the center; C. View from the sea of Posillipo sea cliffs with part of Rosebery Villa built on the top; D. View from the sea of Castel dell' Ovo.

coast with an almost stable coastline position slightly prograding (Calderoni & Russo, 1998).

Posillipo hill during the 1st century BC was constituted by a continuous 6-km long rocky coast mainly made in Neapolitan Yellow Tuff (Deino et al., 2004), which was characterized by the presence of several submerged platforms (Caporizzo et al., 2021) on which different maritime villas and infrastructures were built. It hosted the huge complex of *Pausilypon* Villa, built on various terraces sloping down toward

the sea, on both sides of the Gaiola valley. It extended from west of Trentaremi bay to east of the Marechiaro area, also including the so-called Palazzo degli Spiriti and the Nisida and Marechiaro harbors annexed to the villa (Gunther, 1913; Simeone & Masucci, 2009).

Nisida island (Figure 6A), a tuff cone formed during the last stages of the 3rd eruptive epoch of Campi Flegrei (3.8 ka BP Smith et al., 2011), was already shaped in a sheltered bay due to the marine erosion of its south-western flank. It hosted a port connected to the mainland by an isthmus crossed by a tunnel. The remains of a Roman *pila* (ID#18, Table 4; Mattei et al., 2018b) belonging to the port and those of the fish tanks of *Pausilypon* Villa (ID#19, Table 4; Pagano, 1980), close to the modern Gaiola Island, helped in the establishment of the coastline position during the 1st century century BC and the evaluation of a coastal retreat since that time with maximum values of about 0.2 km that led to the formation of the present island.

Moving NE, the fascinating coastal landscape was articulated in a rugged coastline with sheltered small bays. The first part was characterized by a northeast-southwest orientation and the presence of different structures, including Palazzo degli Spiriti, Marechiaro port (Figure 6B), and Rosebery Villa (ID#20-28, Table 4), and a second one, extending toward Chiaia-Municipio Plain, with a more pronounced NS orientation.

During the Roman period, a supposedly sudden 2-meter subsidence of volcano-tectonic origin produced a decametric coastal retreat that induced the restoration of all the coastal structures (Aucelli et al., 2018). After that time, while the southern sector was not affected by a significant coastline migration during the last 2.0 ka, with the exception of Posillipo Cape (Figure 6C) which suffered a sea-cliff retreat of about 0.2 km, the northernmost was affected by an average coastal retreat with maximum values of about 0.1 km.

Further East, the Chaia-Municipio plain appeared strongly anthropized due to the construction, during the 4th century BC, of the huge *Neapolis* harbor and several maritime villas, like the one on the islet of *Megaris* (nowadays Castel dell'Ovo, Figure 6D; Pappone et al., 2019). Traces of dredging (Di Donato et al., 2018) in the port basin suggest continuous human interventions to counteract the general prograding trend of this low sandy coast with a length and a width of about 2.3 and 0.1 km,

While Chaia-Municipio Plain exhibited a general coastal progradation that reached 1.6 km after the Roman period, the area of Pizzofalcone promontory and the facing *Megaris* Islet has been characterized by a coastal retreat as testified by the presence of paleo-shore platforms extending 25–30 m seaward on which an ancient fish tank was located (ID#29, Table 4), probably related to the presence of the *Lucullus* Villa on the small island.

4. Conclusion

The paleo-environmental reconstruction obtained in this study underlines the complex interaction between the volcano-tectonic activity and glacio-idro-isostatic sea-level rise, occurred in the last 2000 years, that has resulted in substantial coastal changes interesting both the outer and inner parts of Campi Flegrei caldera. On the other hand, the adoption of a transdisciplinary approach aimed at collecting high-resolution data on the ancient RSLs through a multi-proxy analysis overlaid with extensive mapping from morpho-acoustic and optical surveys led to obtaining robust interpretations of the ancient coastal conformation.

In conclusion, this map represents a useful cartographic product to understand the potential coastal trends of an active volcanic area under the interplayed effects of volcanic-tectonic landmass movements and ongoing climate changes.

Acknowledgments

The authors sincerely thank Alberto Greco, Ferdinando Sposito, Luigi De Luca, and Alberto Giordano for their precious support during the marine surveys. Sincere thanks are also due to the 2nd Nucleo Operatori Subacquei of Coast Guard of Naples for the highly specialized support during all phases of the direct and indirect marine surveys. The Ministry of the Environment kindly provided the coastal LIDAR data used as a basemap. The location of some archaeological sites reported in the main Maps was derived from the ArcheoFlegrei website (https://www.archeoflegrei.it/carta-archeologica-dei-campi-flegrei/) and the Gruppo Archeologico Napoletano (https://www.ganapoletano.it/archemail/napolisiti.htm).

Disclosure statement

No potential conflict of interest was reported by the author(s).

Software

The map presented in this work has been produced using Esri ArcGis 10.4 © for the vector and raster datasets, and Corel Draw 2021 © for the editing.

Data availability statement

Data available within the article or its supplementary materials.

ORCID

Gaia Mattei http://orcid.org/0000-0003-4582-3265
Claudia Caporizzo http://orcid.org/0000-0002-8634-6066
Gerardo Pappone http://orcid.org/0000-0001-7424-2908
Alessia Sorrentino http://orcid.org/0000-0002-8636-6454
Paolo Stocchi http://orcid.org/0000-0002-1377-3817
Salvatore Troisi http://orcid.org/0000-0002-4311-6156
Pietro P.C. Aucelli http://orcid.org/0000-0002-8855-6171

References

Amato, V., Aucelli, P. P. C., Mattei, G., Pennetta, M., Rizzo, A., Rosskopf, C. M., & Schiattarella, M. (2018). A geodatabase of Late Pleistocene-Holocene palaeo sea-level markers in the Gulf of Naples. *Alpine and Mediterranean Quaternary*, *31*, 5–9.

Amato, L., Evangelista, A., Nicotera, M. V., & Viggiani, C. (2000). The Crypta Neapolitana; a Roman tunnel of the early imperial age. In *More than two thousand years in the history of architecture*. UNESCO-ICOMOS Internationl Congress.

Amato, V., & Gialanella, C. (2013). New evidences on the Phlegraean bradyseism in the area of Puteolis harbour. In E. Bilotta, A. Flora, S. Lirer & C. Viggiani (Eds.), *Geotechnical engineering for the preservation of monuments and historic sites*. Taylor & Francis Group, London, UK.

Ascione, A., Aucelli, P. P. C., Cinque, A., Di Paola, G., Mattei, G., Ruello, M., Russo Ermolli, E., Santangelo, N., & Valente, E. (2020). Geomorphology of Naples and the Campi Flegrei: Human and natural landscapes in a restless land. *Journal of Maps*, https://doi.org/10.1080/17445647.2020.1768448

Aucelli, P., Brancaccio, L., & Cinque, A. (2017b). Vesuvius and Campi Flegrei volcanoes. Activity, landforms and impact on settlements. In M. Soldati, & M. Marchetti (Eds.), *Landscapes and landforms of Italy* (pp. 389–398). Springer International Publishing. https://doi.org/10.1007/978-3-319-26194-2_33

Aucelli, P. P. C., Cinque, A., Mattei, G., & Pappone, G. (2017a). Late Holocene landscape evolution of the gulf of Naples (Italy) inferred from geoarchaeological data. *Journal of Maps*, *13*(2), 300–310. https://doi.org/10.1080/17445647.2017.1300611

Aucelli, P. P. C., Cinque, A., Mattei, G., Pappone, G., & Rizzo, A. (2019). Studying relative sea level change and correlative adaptation of coastal structures on submerged Roman time ruins nearby Naples (southern Italy). *Quaternary International*, *501*, 328–348. https://doi.org/10.1016/j.quaint.2017.10.011

Aucelli, P. P. C., Cinque, A., Mattei, G., Pappone, G., & Stefanile, M. (2018). Coastal landscape evolution of Naples (Southern Italy) since the Roman period from archaeological and geomorphological data at Palazzo degli Spiriti site. *Quaternary International*, *483*, 23–38. https://doi.org/10.1016/j.quaint.2017.12.040

Aucelli, P. P. C., Mattei, G., Caporizzo, C., Cinque, A., Amato, L., Stefanile, M., & Pappone, G. (2021). Multiproxy analysis of relative sea-level and paleoshoreline changes during the last 2300 years in the Campi Flegrei caldera, Southern Italy. *Quaternary International*, *602*, 110–130. https://doi.org/10.1016/j.quaint.2021.03.039

Aucelli, P. P. C., Mattei, G., Caporizzo, C., Cinque, A., Troisi, S., Peluso, F., Stefanile, M., & Pappone, G. (2020). Ancient Coastal changes due to ground movements and human interventions in the Roman Portus Julius (Pozzuoli Gulf, Italy): Results from photogrammetric and direct surveys. *Water*, *12*, 658. https://doi.org/10.3390/w12030658

Bellucci, F., Woo, J., Kilburn, C. R., & Rolandi, G. (2006). Ground deformation at Campi Flegrei, Italy: Implications for hazard assessment. *Geological Society, London, Special Publications*, *269*(1), 141–157. https://doi.org/10.1144/GSL.SP.2006.269.01.09

Benini, A. (2004). Storia, Archeologia e tutela dei beni archeo logici sommersi: l'esempio dei Campi Flegrei. Giacobelli (a cura di), *Lezioni Fabio Faccenna "Conferenze di Archeologia Subacquea III-V ciclo*, Bari, Italy, pp. 35–43.

Benini, A., Ferrari, G., & Lamagna, R. (2008). Le peschiere di Lucullo (Miseno-Napoli). Atti VI Convegno Nazionale di Speleologia in Cavità Artificiali - OPERA IPOGEA 1/2; Napoli, IT, 159–168.

Benini, A., & Lanteri, L. (2010). Il porto romano di *Misenum*: nuove acquisizioni. In: Ricoveri per navi militari nei porti del Mediterraneo antico e medievale - Atti del Workshop, 4-5 novembre, Ravello, Italy.

Brandon, C. J., Hohlfelder, R. L., & Oleson, J. P. (2008). The concrete construction of the Roman harbours of Baiae and Portus Iulius, Italy: The ROMACONS 2006 field season. *IJNA*, *37*(2), 374–392. https://doi.org/10.1111/j.1095-9270.2008.00191.x

Budillon, F., Amodio, S., Contestabile, P., Alberico, I., Innangi, S., & Molisso, F. (2020). The present-day nearshore submarine depositional terraces off the Campania coast(South-eastern Tyrrhenian Sea): an analysis of their morpho-bathymetric variability. 2020 IMEKO TC-19 International Workshop on Metrology for the SeaAt: Naples, Italy.

Buonaguro, S. (2008). Il sacello degli Augustali di Miseno. Un pavimento 'sommerso'. In *Atti del XIII colloquio dell'Associazione Italiana per lo Studio e la Conservazione del Mosaico*, pp. 175–186, 21-24 febbraio 2007, Canosa di Puglia, Italy.

Busen, T. (2016). L'odeon della Villa Imperiale del Pausilypon: nuove ricerche sulla progettazione architettonica in epoca romana. In G. Camodeca & M. Giglio, *PUTEOLI. Studi di storia ed archeologia dei Campi Flegrei*. Università degli Studi di Napoli L'Orientale, Napoli, Italy.

Calderoni, G., & Russo, F. (1998). The geomorphological evolution of the outskirts of Naples during the Holocene: A case study of the Bagnoli-Fuorigrotta depression. *The Holocene*, *8*(5), 581–588. https://doi.org/10.1191/095968398671591932

Camodeca, G. (1994). Puteoli porto annonario e il commercio del grano in età imperiale. *Publications de l'École française de Rome*, *196*(1), 103–128.

Camodeca, G. (2011). Nuove dediche imperiali dal collegio degli Augustales di Miseno per Domiziano e per Elagabalo. In *Corolla Epigraphica. Hommages Y. Burnand* (pp. 374–391). Bruxelles.

Caporizzo, C., Aucelli, P. P. C., Di Martino, G., Mattei, G., Tonielli, R., & Pappone, G. (2021). Geomorphometric analysis of the natural and anthropogenic seascape of Naples (Italy): A high-resolution morpho-bathymetric survey. *Transaction in GIS*, *25*(5), 2571–2595. https://doi.org/10.1111/tgis.12829

Caputo, P. (2006). Ricerche sul suburbio meridionale di Cuma. Ricerche sul suburbio meridionale di Cuma, 107–134.

Cinque, A., Aucelli, P. P. C., Brancaccio, L., Mele, R., Milia, A., Robustelli, G., Romano, P., Russo, F., Russo, M., Santangelo, N., & Sgambati, D. (1997). *Guide for the excursion "Volcanism, tectonics and recent geomorphological change in the Bay of Napoli"*. Fourth International Conference on Geomorphology, Bologna, Italy, 28 August - 3 September, 1997.

de Boer, B., Stocchi, P., & Van De Wal, R. (2014). A fully coupled 3-D ice-sheet-sea-level model: Algorithm and applications. *Geoscientific Model Development*, *7*(5), 2141–2156. https://doi.org/10.5194/gmd-7-2141-2014

Di Fraia, G. (1993). Baia sommersa. Nuove evidenze topografiche e monumentali. Archeologia subacquea. In

Studi, ricerche e documenti, I (pp. 21–48). Università degli Studi della Tuscia-Viterbo, Roma, IT.

Di Fraia, G., Lombardo, N., & Scognamiglio, E. (1986). Contributi alla topografia di Baia sommersa. *Puteoli - Studi di Storia Antica 9-10*, 211–229.

Deino, A. L., Orsi, G., Piochi, M., & de Vita, S. (2004). The age of the Neapolitan Yellow Tuff caldera-forming eruption (Campi Flegrei caldera – Italy) assessed by 40Ar/39Ar dating method. *Journal of Volcanology and Geothermal Research*, *185*, 48–56. https://doi.org/10.1016/S0377-0273(03)00396-2

De Pippo, T., Donadio, C., Pennetta, M., Terlizzi, F., & Valente, A. (2007). Genesis and morphological evolution of fusàro lagoon (Campania, southern Italy) in the Holocene. *Bollettino Della Società Geologica Italiana*, *126*(1), 89.

Di Donato, V., Ruello, M. R., Liuzza, V., Carsana, V., Giampaola, D., Di Vito, M. A., Morhange, C., Cinque, A., & Russo Ermolli, E. (2018). Development and decline of the ancient harbor of Neapolis. *Geoarcheaology*, *33*(5), 542–557. https://doi.org/10.1002/gea.21673

Di Vito, M., Lirer, L., Mastrolorenzo, G., & Rolandi, G. (1987). The 1538 Monte Nuovo eruption (Campi Flegrei, Italy). *Bulletin of Volcanology*, *49*(4), 608–615. https://doi.org/10.1007/BF01079966

Dvorak, J. J., & Mastrolorenzo, G. (1991). The mechanisms of recent vertical crustal movements in Campi Flegrei Caldera, southern Italy. *USGS, Special Paper*, *263*, 1–47.

Gianfrotta, P. A. (2011). La topografia sulle bottiglie di Baia. *Rivista di archeologia*, *35*, 13–40.

Gianfrotta, P. A. (2012). Ricerche nell'area sommersa del "Portus Iulius" (1988-'90 e successive): Un riepilogo. *Atlante Temat. Topogr. Antica 22*, 1–20.

Guadagno, G. (1994). Il sacello degli augustali di Miseno. In M. O. Jentel & G. Deschênes-Wagner (Eds.), *Tranquillitas. Mélanges en l'honneur de Tran tam Tinh* (pp. 243–253). Université Laval.

Guidone, I., Guarino, P. M., & Damiano, N. (2017). *Publication Preview Source Analisi contestuale di cavità di origine antropica nel Parco Archeologico delle Terme di Baia (Campania, Italia)*. Cavità Di Origine Antropica, Modalità d'Indagine, Aspetti Di Catalogazione, Analisi Delle Pericolosità, Monitoraggio e Valorizzazione, Roma, Italy, 1. Dicembre, 2017.

Gunther, R. T. (1913). *Pausilypon, the imperial villa near Naples: With a description of the submerged foreshore and with observations on the tomb of Virgil and on other Roman antiquities on Posilipo*.

Iliano, G. (2017). Misenum: The harbour and the city. Landscapes in context. *Archeologia e Calcolatori*, *28*(2), 379–389.

Isaia, R., Iannuzzi, E., Sbrana, A., & Marianelli, P. (2016). Note Illustrative della Carta Geologica d'Italia alla scala 1: 50.000, Foglio 446-447 Napoli (aree emerse).

Isaia, R., Vitale, S., Marturano, A., Aiello, G., Barra, D., Ciarcia, S., Iannuzzi, E., & Tramparulo, F. (2019). High-resolution geological investigations to reconstruct the long-term ground movements in the last 15 kyr at Campi Flegrei caldera (southern Italy). *Journal of Volcanology and Geothermal Research*, *385*, 143–158. https://doi.org/10.1016/j.jvolgeores.2019.07.012

Levi, D. (1969). *Enciclopedia dell'arte antica, Classica e Orientale*. Instituto della Enciclopedia Italiana.

Lombardo, N. (2009). Baia: le terme sommerse a Punta dell'Epitaffio. Ipotesi di ricostruzione volumetrica e creazione di un modello digitale. Archeologia e calcolatori, 20, 373–396.

Maiuri, A. (1963). Passeggiate in Magna Grecia. L'Arte Tipografica Napoli.

Maniscalco, F. (2004). Il Parco Sommerso di Baia. In F. Maniscalco (Ed.), *Tutela, conservazione e valorizzazione del Patrimonio Culturale Subacqueo* (pp. 195–202). Massa Editore, Napoli, Italy.

Mattei, G., Aucelli, P. P. C., Caporizzo, C., Peluso, F., Pappone, G., & Troisi, S. (2020a). Innovative Technologies for Coastal Paleo-Landscape Reconstruction and Paleo-Sea Level Measuring. In C. Parente, S. Troisi, & A. Vettore (Eds.), *R3 in geomatics: Research, results and review. R3GEO 2019. Communications in computer and information science* (pp. 1246). Springer. https://doi.org/10.1007/978-3-030-62800-0

Mattei, G., Aucelli, P. P. C., Caporizzo, C., Rizzo, A., & Pappone, G. (2020b). New geomorphological and historical elements on Morpho-Evolutive trends and relative Sea-level changes of Naples Coast in the last 6000 years. *Water*, *12*(9), 2651. https://doi.org/10.3390/w12092651

Mattei, G., Caporizzo, C., Corrado, G., Vacchi, M., Stocchi, P., Pappone, G., Schiattarella, M., & Aucelli, P. P. C. (2022). On the influence of vertical ground movements on Late-Quaternary sea-level records. A comprehensive assessment along the mid- Tyrrhenian coast of Italy (Mediterranean Sea). *Quaternary Science Reviews*, *279*, 107384. https://doi.org/10.1016/j.quascirev.2022.107384

Mattei, G., Troisi, S., Aucelli, P. P. C., Pappone, G., Peluso, F., & Stefanile, M. (2018a). Multiscale reconstruction of natural and archaeological underwater landscape by optical and acoustic sensors. IEEE International Workshop on Metrology for the Sea, Bari, Italy. https://doi.org/10.1109/MetroSea.2018.8657872

Mattei, G., Troisi, S., Aucelli, P. P. C., Pappone, G., Peluso, F., & Stefanile, M. (2018b). Sensing the submerged landscape of Nisida Roman Harbour in the Gulf of Naples from integrated measurements on a USV. *Water*, *10* (11), 1686. https://doi.org/10.3390/w10111686

Miniero, P. (2010a). La villa romana nel Castello di Baia: un riesame del contesto. *Mélanges de l'École française de Rome-Antiquité*, *122*(2), 439–450.

Miniero, P. (2010b). Baia sommersa e portus Iulius. Il rilievo con strumentazione integrata Multibeam. In D. J. Blackman & M C. (Eds.), *Ricoveri Per Navi Militari Nei Porti del Mediterraneo Antico e Medievale* (pp. 101–108). Edipuglia.

Morhange, C., Bourcier, M., Laborel, J., Giallanella, C., Goiran, J. P., Crimaco, L., & Vecchi, L. (1999). New data on historical relative sea level movements in Pozzuoli, Phlaegrean fields, southern Italy. *Physics and Chemistry of the Earth, Part A: Solid Earth and Geodesy*, *24*(4), 349–354. https://doi.org/10.1016/S1464-1895(99)00040-X

Morhange, C., Marriner, N., Laborel, J., Todesco, M., & Oberlin, C. (2006). Rapid sea-level movements and non-eruptive crustal deformation in the phlegrean fields caldera, Italy. *Geology*, *34*(2), 93–96. https://doi.org/10.1130/G21894.1

Pagano, M. (1980). Gli impianti marittimi della villa Pausilypon. Puteoli. *Studi di storia antica*, *4*, 245–255.

Paget, R. F. (1971). From Baiae to Misenum. *Vergilius*, *17*, 22–38.

Paoli, P. A. (1768). Avanzi delle antichita esistenti a Pozzuoli Cuma e Baia Antiquitatum Puteolis Cumis Baiis existentium reliquiae.

Pappalardo, U., & Russo, F. (2001). Il bradisismo dei Campi Flegrei (Campania): dati geomorfologici ed evidenze archeologiche. In: Gianfrotta, P.A., Maniscalco, F.,

(Eds.), Forma Maris. Forum Internazionale di Archeologia Subacquea, Pozzuoli (Napoli), 22–24 settembre 1998, 107–129. Massa Editore, Napoli.

Pappone, G., Aucelli, P. P. C., Mattei, G., Peluso, F., Stefanile, M., & Carola, A. (2019). A detailed reconstruction of the Roman landscape and the submerged archaeological structure at "Castel dell'Ovo islet" (Naples, Southern Italy). *Geosciences*, *9*(4), 170. https://doi.org/10.3390/geosciences9040170

Parascandola, A. (1947). I Fenomeni Bradisismici del Serapeo di Pozzuoli, Napoli. *Guida: Napoli, Italy*.

Passaro, S., Barra, M., Saggiomo, R., Di Giacomo, S., Leotta, A., Uhlen, H., & Mazzola, S. (2013). Multi-resolution morphobathymetric survey results at the Pozzuoli-Baia underwater archaeological site (Naples, Italy). *Journal of Archaeological Science*, *40*(2), 1268–1278. https://doi.org/10.1016/j.jas.2012.09.035

Peltier, W. R. (2004). Global Glacial Isostasy and the Surface of the Ice-Age Earth: The ICE-5G(VM2) model and GRACE. *Annual Review of Earth and Planetary Sciences*, *32*(1), 111–149. https://doi.org/10.1146/annurev.earth.32.082503.144359

Peltier, W. R., Argus, D. F., & Drummond, R. (2015). Space geodesy constrains ice-age terminal deglaciation: The global ICE-6G_C (VM5a) model. *Journal of Geophysical Research: Solid Earth*, *120*(1), 450–487. https://doi.org/10.1002/2014JB011176

Shennan, I. (2015). Handbook of sea-level research: Framing research questions. In I. Shennan, A. J. Long, & B. P. Horton (Eds.), *Handbook of Sea-level research* (pp. 3–25). John Wiley & Sons. https://doi.org/10.1002/9781118452547

Simeone, M., & Masucci, P. (2009). Analisi geoarcheologiche nell'Area Marina Protetta Parco Sommerso di Gaiola (Golfo di Napoli). *Alpine and Mediterranean Quaternary*, *22*(1), 25–32.

Smith, V. C., Isaia, R., & Pearce, N. J. C. (2011). Tephrostratigraphy and glass compositions of post-15 kyr campi. Flegrei eruptions: Implications for eruption history and chronostratigraphic markers. *Quaternary Science Reviews*, *30*(25–26), 3638–3660. https://doi.org/10.1016/j.quascirev.2011.07.012

Spada, G., & Stocchi, P. (2007). SELEN: A Fortran 90 program for solving the "Sea Level Equation". *Computers and Geosciences*, *33*(4), 538. https://doi.org/10.1016/j.cageo.2006.08.006

Todesco, M., Costa, A., Comastri, A., Colleoni, F., Spada, G., & Quareni, F. (2014). Vertical ground displacement at Campi Flegrei (Italy) in the fifth century: Rapid subsidence driven by pore pressure drop. *Geophysical Research Letters*, *41*(5), 1471–1478. https://doi.org/10.1002/2013GL059083

Troise, C., De Natale, G., Pingue, F., Obrizzo, F., De Martino, P., Tammaro, U., & Boschi, E. (2007). Renewed ground uplift at Campi Flegrei caldera (Italy): New insight on magmatic processes and forecast. *Geophysical Research Letters*, *34*(3), 3. https://doi.org/10.1029/2006GL028545